Canonical Notch signaling in the developing lung is required for determination of arterial smooth muscle cells and selection of Clara versus ciliated cell fate

Mitsuru Morimoto[1], Zhenyi Liu[1], Hui-Teng Cheng[2], Niki Winters[3], David Bader[3] and Raphael Kopan[1,*]

[1]Department of Developmental Biology and Division of Dermatology, Washington University School of Medicine, Box 8103, Saint Louis, MO 63110-1095, USA
[2]Department of Internal Medicine, Far Eastern Memorial Hospital and National Taiwan University Hospital, Taipei, Taiwan
[3]Stahlman Cardiovascular Research Laboratories, Program for Developmental Biology, and Department of Medicine, Vanderbilt University Medical Center, Nashville, TN 37232-6300, USA
*Author for correspondence (kopan@wustl.edu)

Accepted 23 October 2009
Journal of Cell Science 123, 213-224 Published by The Company of Biologists 2010
doi:10.1242/jcs.058669

Summary

Lung development is the result of complex interactions between four tissues: epithelium, mesenchyme, mesothelium and endothelium. We marked the lineages experiencing Notch1 activation in these four cellular compartments during lung development and complemented this analysis by comparing the cell fate choices made in the absence of RBPjκ, the essential DNA binding partner of all Notch receptors. In the mesenchyme, RBPjκ was required for the recruitment and specification of arterial vascular smooth muscle cells (vSMC) and for regulating mesothelial epithelial-mesenchymal transition (EMT), but no adverse affects were observed in mice lacking mesenchymal RBPjκ. We provide indirect evidence that this is due to vSMC rescue by endothelial-mesenchymal transition (EnMT). In the epithelium, we show that Notch1 activation was most probably induced by Foxj1-expressing cells, which suggests that Notch1-mediated lateral inhibition regulates the selection of Clara cells at the expense of ciliated cells. Unexpectedly, and in contrast to *Pofut1*-null epithelium, Hes1 expression was only marginally reduced in *RBPjκ*-null epithelium, with a corresponding minimal effect on pulmonary neuroendocrine cell fate selection. Collectively, the primary roles for canonical Notch signaling in lung development are in selection of Clara cell fate and in vSMC recruitment. These analyses suggest that the impact of γ-secretase inhibitors on branching in vitro reflect a non-cell autonomous contribution from endothelial or vSMC-derived signals.

Key words: Notch, Lung, Clara cells, Ciliated cells, Arterial vascular smooth muscle cells

Introduction

Lung development is orchestrated by complex mesenchymal-epithelial interactions that coordinate the temporal and spatial expression of multiple regulatory factors that are required for proper organ formation. Distinct populations of stem cells contribute to the epithelial and mesenchymal compartments (Mailleux et al., 2005; Perl et al., 2002; Rawlins et al., 2007; Rock et al., 2009). In the tracheal epithelium, the basal cell generates mucous cells, Clara (secretory) and ciliated cells (Hong et al., 2004; Rock et al., 2009). Smaller bronchi contain the latter two cell types and pulmonary neuroendocrine cells (PNECs). The distal-most airway, the alveolus, is lined with thin layers of flat Type I cells and cuboidal Type II cells (Kimura and Deutsch, 2007; Rawlins and Hogan, 2006). At the pseudoglandular stage (E11.5-16.5), during which most of airway branching morphogenesis takes place, it is thought that the terminal buds contain a population of multipotent epithelial progenitors (Perl et al., 2005). As the bronchial tree extends, descendants of these cells give rise to lineage-restricted progenitors that produce Clara and ciliated cells (and possibly other cell types) in the conducting airways (Cardoso and Lu, 2006; Perl et al., 2002).

The lung mesenchyme is comprised of multiple cell types, including connective tissue, endothelial cells, lymphatics, smooth muscle cells surrounding airways and blood vessels, myofibroblasts involved in septum formation, and cartilage-forming cells in the trachea. In addition, pleura-derived mesothelial cells cover the outer surface of the lung. The developmental origin of these cells is a matter of some dispute (Hall et al., 2000), with most cells believed to be derived from the splanchnic mesenchyme, whereas other cells (endothelial, smooth muscle) are believed to invade the lung as it expands (Cardoso and Lu, 2006; Galambos and Demello, 2007; Hall et al., 2000). Although bronchial smooth muscle cells (bSMCs) are derived from a distal lung mesenchyme lineage expressing fibroblast growth factor 10 (FGF10) (Mailleux et al., 2005), vSMCs are thought to derive from an invading population (Hall et al., 2000).

Evidence demonstrating the importance of Notch signaling in the developing respiratory system is rapidly growing. Mice that are genetically deficient in Hes1, a target of Notch signaling in several biological systems, show hyperplasia of PNECs and a decreased number of Clara cells, suggesting the bi-potential precursors of Clara and ciliated cells are separated from PNEC precursors via a Notch-mediated lateral inhibition feedback loop (Ito et al., 2000; Shan et al., 2007). As this manuscript was being prepared for publication, a role for Notch signaling as a suppressor of the ciliated cell fate was reported (Guseh et al., 2009; Tsao et al., 2009). Induced expression of a constitutively active Notch1 intracellular domain (N1ICD) in lung epithelial cells throughout development promoted mucous metaplasia and remarkably decreased the number of ciliated cells (Guseh et al., 2009). Conditional removal of Pofut1, a glycosyltransferase required for Notch signaling and possibly other cellular functions (Kopan and Ilagan, 2009), promoted ciliated cell expansion at the expense of Clara cells (Tsao et al., 2009). Interestingly, airway branching morphology was not altered by loss

of Notch signaling in the epithelium, despite previous loss-of-function reports demonstrating enhanced branching when lung anlagen were cultured in the presence of γ-secretase inhibitors (GSI) (Tsao et al., 2008) or antisense *Notch1* oligonucleotides (Kong et al., 2004). The discrepancy between in vivo and in vitro loss of function analyses might be explained by an unknown function for Notch signaling in lung mesenchyme.

Although these observations strongly suggest a role for Notch signaling in the developing lung, several caveats limit our ability to identify the cells in which Notch receptors function, and which specific receptor(s) contribute to lung organogenesis. Overexpression of N1ICD (Guseh et al., 2009) exposed the tissue to non-physiological levels of Notch pathway activation in both the level and duration of the signal. Moreover, given that Hes1 can respond to other signaling pathways (Yoshiura et al., 2007), notably FGF (Nakayama et al., 2008), its activation might not depend on Notch in every cellular context (Lee et al., 2007). To look at which specific cell types require Notch activity during lung morphogenesis, and to begin to assign functions to specific receptors, we examined the role of Notch signaling in different compartments throughout lung development. Given the dominant role suggested for Notch1, we wished to visualize the lineages derived from cells experiencing Notch1 activation. To map these lineages, we modified *N1IP::CRE^{LOW}* (Notch1 Intramembrane Proteolysis) (Vooijs et al., 2007) to generate the *N1IP::CRE^{HI}* knock-in mouse strain in which Cre activity was improved, thus increasing detection sensitivity. These experiments were followed by detection of N1ICD with epitope-specific antibodies to observe sites of Notch1 activity. Finally, genetic inactivation of the canonical Notch pathway in epithelia or jointly in the mesenchyme and mesothelium was achieved by removal of RBPjκ, the DNA binding partner of all four Notch receptors and a core component of canonical Notch signaling (Kopan and Ilagan, 2009); more specifically, RBPjκ is essential for Notch-mediated Hes1 activation. We uncovered a specific function for Notch signaling in the specification of the pulmonary vSMCs and in mesothelial epithelial-mesenchymal transition (EMT). We confirmed the function of Notch in selection of Clara or ciliated cell fate and extended these observations, demonstrating a lateral inhibitory role for Notch1 in this process and during Clara cell regeneration.

Results

Notch1 activation in lung mesenchyme is restricted to specific lineages

In vivo fate mapping of cells that experienced Notch1 activation with *N1IP::CRE^{LOW}* allows identification of lineages in which Notch1 activity might be required (Vooijs et al., 2007). To enhance our ability to image such lineages in the lung, we generated *N1IP::CRE^{HI}* knock-in mice in which Cre recombinase [instead of Cre–6-Myc-Tag (Cre-6MT)] replaced the Notch1 intracellular domain. Ligand binding unfolds a negative regulatory domain, triggers ectodomain shedding and enables γ-secretase-mediated proteolysis of the Notch transmembrane domain. This leads to the release of Cre (Vooijs et al., 2007). When combined with a strain carrying a conditional reporter, Cre-mediated excision of a loxP-flanked 'stop' cassette constitutively activates reporter expression and indelibly marks cells that experienced Notch activation and all of their progeny. In *N1IP::CRE^{LOW}*, the inefficient Cre-6MT marks only a subset of cells (those experiencing moderate to high levels of sustained Notch activity, such as endothelium) (Vooijs et al., 2007), whereas the new *N1IP::CRE^{HI}, R26R* strain marked cells receiving moderate-to-low levels of Notch activity and therefore increased coverage of Notch1 activation patterns [a full description of this line will be provided elsewhere, but compare the lung image shown here and in Vooijs et al. (Vooijs et al., 2007)]. We used *N1IP::CRE^{HI}, R26R* mice to determine which lineages within the lung experienced Notch1 activation during development.

Scattered, β-galactosidase-labeled mesenchymal (Fig. 1A) and mesothelial cells (black arrowhead in Fig. 1A,B) were detected in the lung mesenchyme at E13.5 in *N1IP::CRE^{HI}, R26R* mice. As the lung matured, the number of these cells increased (Fig. 1A,C,D). To identify which mesenchymal cell types were derived from cells experiencing Notch1 activation, we co-immunostained tissue sections with anti-β-galactosidase and cell-type-specific antibodies (SM22α, PECAM, SMA). The *N1IP::CRE^{HI}* reporter abundantly marks the vascular plexus (Fig. 1I-N) and both arterial endothelial cells and vSMCs (gray arrowheads in Fig. 1O-Q). By contrast, β-galactosidase was not activated in bSMCs (Fig. 1G, white arrowheads in Fig. 1O-Q) or myofibroblasts located at the tip of the alveolar septum (white arrowheads in Fig. 1R-T). These data suggest that by E18.5, the descendents of cells experiencing Notch1 activation contributed extensively if not exclusively to endothelial and vSMC cells.

Notch signaling is required to commit mesenchymal cells to the arterial smooth muscle cell fate

RBPjκ is ubiquitously expressed in lung mesenchyme (Fig. 2A, Fig. 3A). *Dermo1-Cre* (Yu et al., 2003) is expressed within the lung mesenchymal (supplementary material Fig. S1A-C) and mesothelial (see below) lineages; only a few endothelial cells are targeted by this strain and no expression is detected in the epithelium (Yin et al., 2008). To test whether canonical Notch signaling is necessary for mesenchymal lung development, we employed Dermo1-Cre (Yu et al., 2003) to delete floxed *RBPjκ* alleles from the mesenchymal and mesothelial lineages within the developing lung (Drm1-RKO mice). Drm1-RKO mice die within 24 hours due to a highly penetrant ventricular septal defect (VSD; supplementary material Fig. S2). Notably, *Dermo1-Cre* is expressed in the cardiac cushion tissue that is generated by endothelial-mesenchymal transition (EnMT) (Lavine et al., 2008; Timmerman et al., 2004). This indicates an unappreciated requirement for Notch signaling after EnMT has occurred. Importantly, Drm1-RKO pups filled their lungs with air and their breathing was not labored, consistent with normal surfactant expression and lung function in Drm1-RKO mice.

By E10.5, Dermo1-Cre had efficiently deleted *RBPjκ* from mesenchymal and mesothelial cells (Fig. 2B) (Yin et al., 2008), but Drm1-RKO lungs were morphologically indistinguishable from controls (Fig. 2C-H). Clara and Type II cells formed properly (supplementary material Fig. S3A-D), indicating that canonical Notch signaling does not contribute to the complex mesenchymal-epithelial feedback loops required for lung development (White et al., 2007; White et al., 2006; Yin et al., 2008). As expected, epithelial cells (Fig. 3C) and vascular cells retain RBPjκ protein (white arrowheads in Fig. 3D-I) within Drm1-RKO lungs. Because Dermo1-Cre is rarely active in endothelial lineages (supplementary material Fig. S3E-G) (Yu et al., 2003), these observations argue against conversion of lung mesenchyme, which is RBPjκ-depleted at E10.5, to endothelium (Stenmark and Abman, 2005).

To quantify the contribution of the Dermo1-Cre lineage to the vascular and bronchial SMC lineages, we counted cells double-positive for smooth muscle actin and β-galactosidase (SMA$^+$, β-gal$^+$) in arteries and airways of *Dermo1-Cre, R26R* embryos. SMA and SM22α are SMC markers, and β-galactosidase is a lineage

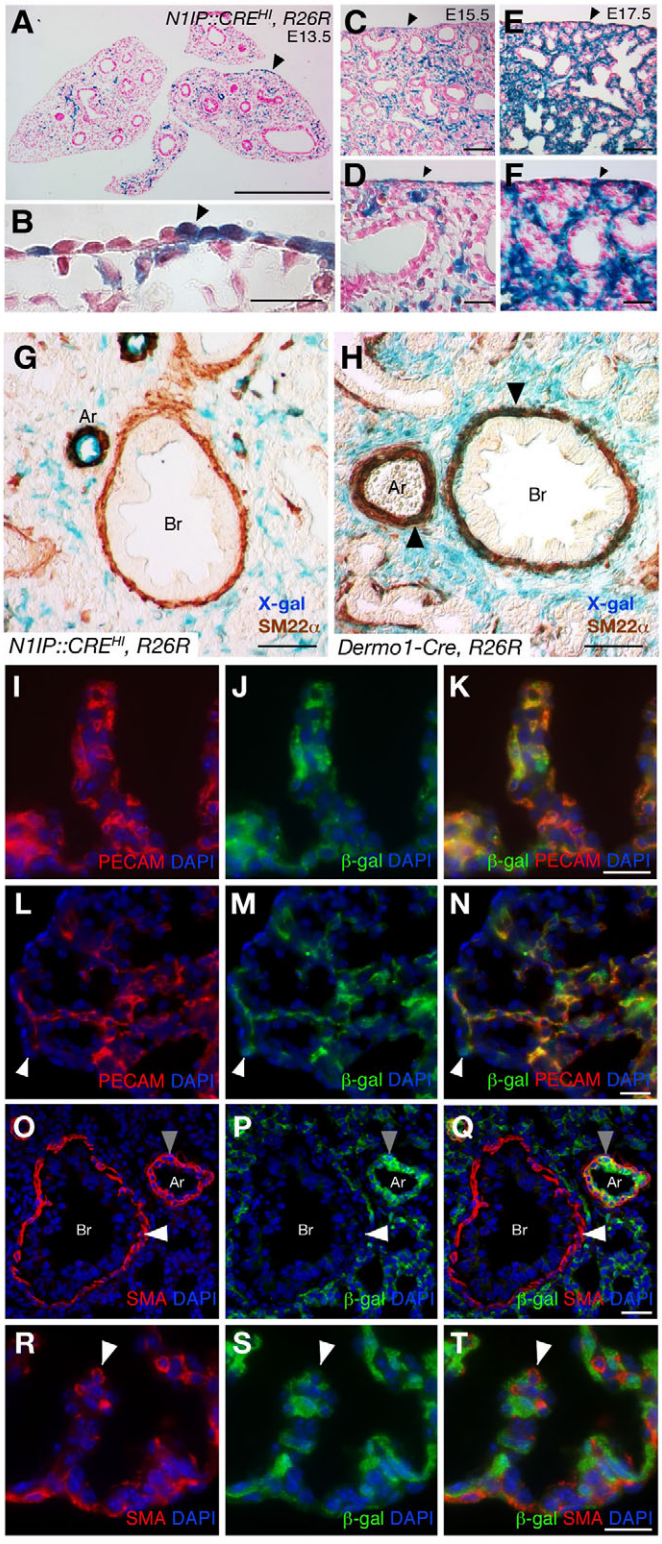

Fig. 1. Mesenchymal cells experiencing Notch1 activation contribute predominantly to the lung vasculature. X-gal staining of *N1IP::CRE^{HI}, R26R* lung sections at E13.5 (**A**,**B**), E15.5 (**C**,**D**) and E17.5 (**E**,**F**). N1IP::CRE^{HI} activity marked several mesenchymal and mesothelial cells (black arrowheads). X-gal and SM22α co-staining of lungs from *N1IP::CRE^{HI}, R26R* (**G**) and *Dermo1-Cre, R26R* (**H**) mice at E15.5. N1IP::CRE^{HI} activity labeled the vasculature but not peripheral bronchi (G), whereas Dermo1-Cre-labeled cells commit to both arterial and bSMCs (H, black arrowheads). Co-immunostaining for β-galactosidase and PECAM (**I-N**) or SMA (O-T) of *N1IP::CRE^{HI}, R26R* lung at E18.5. Distal endothelial (I-K) and mesothelial cells (L-M, white arrowheads) express β-galactosidase. A subset of vSMCs also expresses β-galactosidase (**O-Q**, gray arrowheads); whereas bSMCs (O-Q, white arrowheads) or myofibroblasts in alveolar septa (**R-T**, white arrowheads) do not. Ar, artery; Br, bronchus. Scale bars: A, 0.5 mm; B, 10 μm; C,E, 0.1 mm; D,F, 25 μm; G,H, 50 μm; I-T, 20 μm.

tracer used to quantify the contribution of Drm1-RKO cells to these lineages. To quantify the contribution of RBPjκ-deficient (RBPjκ$^{-/-}$) cells to SMC, we stained for SM22α and RBPjκ proteins (Fig. 3J-L). SM22α^{+}, β-gal^{+} cells and SM22α^{+}, RBPjκ$^{-/-}$ cells contributed equally to bSMC (Fig. 3M; 90% for both β-gal^{+} (gray arrowheads in supplementary material Fig. S1A-C) and RBPjκ$^{-/-}$ cells (gray arrowheads in Fig. 3J-L). The absence of RBPjκ protein from most bSMCs indicated strongly that Notch signaling was dispensable for the execution of the bSMC differentiation program.

In contrast to bSMC, a striking requirement for RBPjκ was observed in vSMC. Whereas most vSMCs (81%) labeled with SM22α and β-galactosidase, indicating a robust contribution from the Dermo1-Cre lineage (Fig. 1H and Fig. 3M; white arrowheads in supplementary material Fig. S1A-C), only 15% of vSMC cells were SM22α^{+}, RBPjκ$^{-/-}$ (Fig. 3J-M); the rest contained RBPjκ protein and therefore must have arisen from outside the *Dermo1-Cre* lineage. This indicates that although canonical Notch signaling was not required for the execution of the bSMC differentiation program, Notch signaling promoted the selection of the vSMC fate. Finally, although the majority of endothelial cells appear to have been derived from outside the *Dermo1*-Cre lineage at E16.5, 21% of the endothelial cells (VEGFR2^{+}) were β-galactosidase-positive and, thus, Dermo1-Cre derived (Fig. 3M; gray arrowheads in supplementary material Fig. S1D-F). Interestingly, the fraction of Dermo1-Cre-derived endothelial cells was reduced in Drm1-RKO lungs (Fig. 3M).

N1IP::CRE mice detect a population of cells, only some of which are engaged in Notch signaling. To look at which cells activated Notch1 within the lung mesenchyme, we used anti-N1ICD antibody to detect Notch1 activation. Double staining for N1ICD and SMA at E14.5 revealed that Notch1 receptor is activated in endothelial cells (Fig. 4A-C, asterisks), vSMCs and in peripheral mesenchymal cells (Fig. 4A-C, white arrowheads) but never in bSMCs (Fig. 4A-C, gray arrowheads). These observations complement the results obtained with the N1IP::CRE^{HI} (Fig. 1), indicating that Notch1 signaling is required for the arterial vSMC fate in developing mesenchyme and not in a general early precursor.

Platelet-derived growth factor receptor (PDGFR)-β is expressed in pericytes, the progenitor for vSMCs (Andrae et al., 2008), where it regulates migration, proliferation and differentiation into vSMC (Jin et al., 2008). We therefore measured the expression level of PDGFR-β in Drm1-RKO mesenchyme at E14.5. PDGFR-β was expressed in the wild-type mesenchyme (Fig. 4D-F) and in RBPjκ-positive cells located within Drm1-RKO mesenchyme (white arrowheads in Fig. 4G-I), but was absent from RBPjκ-negative cells, as judged by immunohistochemistry (gray arrowheads in Fig. 4G-I). Reduced *PDGFR-β* mRNA levels were confirmed by quantitative RT-PCR; expression of endothelial controls (VEGFR1 and 2) was not significantly altered in the same sample at E13.5 (Fig. 4J). Because Notch signaling might also be required for cell proliferation (Sakata et al., 2004; Wang et al., 2003), we assessed cell proliferation by immunohistochemical detection of phospho-histone H3 and

observed no differences in the number of cells positive for phospho-histone H3 between Drm1-RKO and wild-type E14.5 lungs (Fig. 4K-M, white arrow points to a proliferating RBPjκ-negative cell).

Endothelial-mesenchymal transition, but not epithelial-mesenchymal transition of mesothelial cells, might rescue vSMCs in RBPjk-deficient mesenchyme

During this analysis, we noticed that the overall numbers of vSMC in Drm1-RKO lungs did not change, perhaps explaining the normal

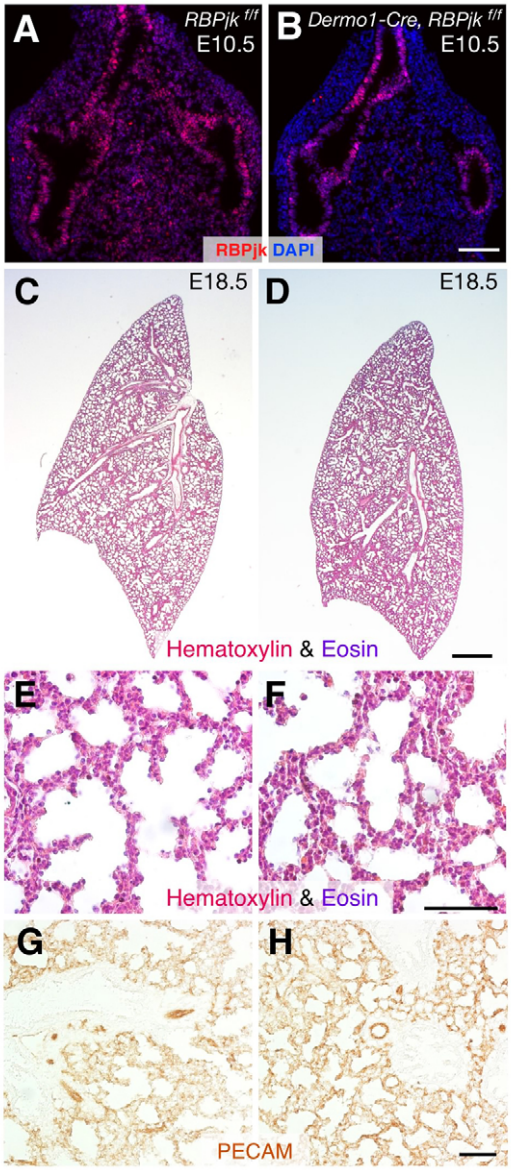

Fig. 2. Ablation of *RBPjκ* in the Dermo1 lineage does not disrupt lung development. Lung sections from E10.5 *RBPjκ*$^{flox/flox}$ (**A**) and *Dermo1-Cre, RBPjκ*$^{flox/flox}$ (**B**) stained for RBPjκ. Note that Dermo1-Cre deleted *RBPjκ* throughout the lung mesenchyme and mesothelium by E10.5 but not the epithelium or endothelium. At E18.5, lung morphology was examined using hematoxylin and eosin staining in *RBPjκ*$^{flox/flox}$ control (**C**,**E**) or *Dermo1-Cre, RBPjκ*$^{flox/flox}$ mutant (**D**,**F**) mice. The morphology of lungs from control and mutant mice is indistinguishable. PECAM staining (brown) revealed normal vascular plexus in both controls (**G**) and mutants (**H**). Scale bars: 100 μm (A,B); 0.5 mm (C,D); 0.1 mm (E-H).

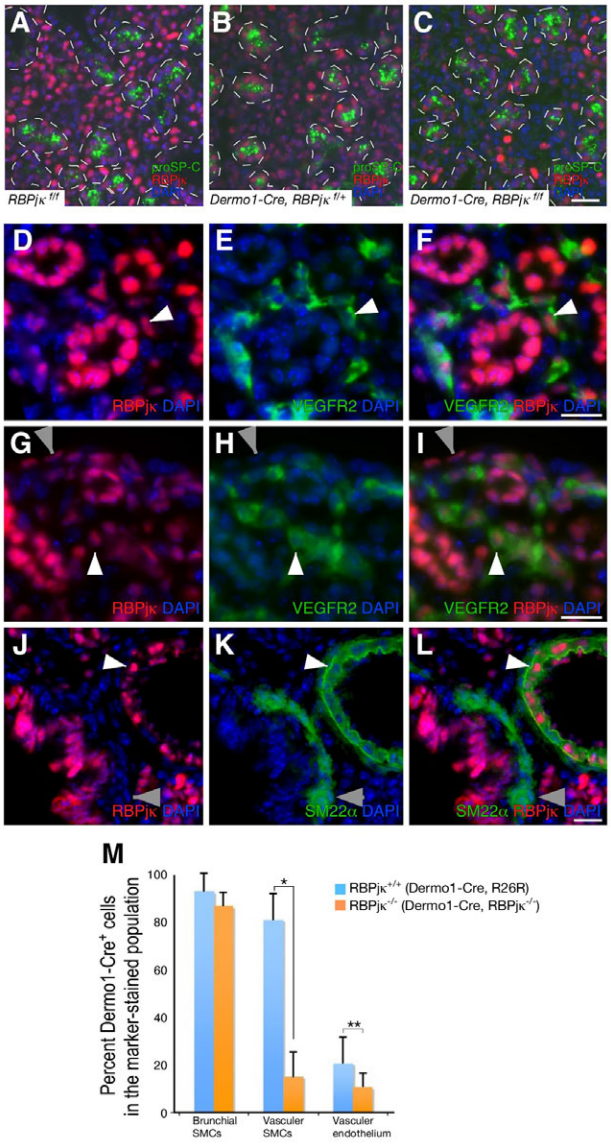

Fig. 3. RBPjκ-deleted mesenchymal cells are excluded from the vSMC fate. Double staining for RBPjκ and proSP-C in *RBPjκ*$^{flox/flox}$ (**A**), *Dermo1-Cre, RBPjκ*$^{+/flox}$ (**B**), *Dermo1-Cre, RBPjκ*$^{flox/flox}$ (**C**) lungs at E16.5. Dashed lines indicate proSP-C-positive epithelial cells. In *Dermo1-Cre, RBPjκ*$^{flox/flox}$ lung mesenchyme, only a few cells were RBPjκ-positive, whereas *RBPjκ*$^{flox/flox}$ and *Dermo1-Cre, RBPjκ*$^{+/flox}$ showed ubiquitous nuclear RBPjκ staining. RBPjκ-positive cells in the mutant lung derived from outside the Dermo1-Cre lineage. (**D-L**) Double staining for RBPjκ and VEGFR2 (D-I) or SM22α (J-L) in the *Dermo1-Cre, RBPjκ*$^{flox/flox}$ lung at E16.5 revealed that mesenchymal RBPjκ staining in the mutant lung colocalized with endothelial cell markers (D-I, white arrowheads) and vascular (J-L, white arrowheads), but not bronchial (J-L, gray arrowheads) SMCs. RBPjκ-positive mesothelial cells were frequently observed in the mutant lung mesothelium (G-I, gray arrowheads). (**M**) Percentage of Dermo1-Cre lineage cells that contributed to SMCs or vascular endothelium. The percentages of RBPjκ-positive (blue) or RBPjκ-negative (orange) cells in distinct *Dermo1-Cre, R26R* lung populations were determined at E16.5 by immunohistochemistry. Six to eight images from each group were taken at 400× magnification, and the number of cells in each population was counted. Whereas statistically identical fractions of RBPjκ-positive and RBPjκ-negative cells contributed to bSMCs, RBPjκ-negative cells contributed significantly less to the vSMCs and vascular endothelium fates in *Dermo1-Cre, RBPjκ*$^{flox/flox}$ lungs. Error bars indicate s.d. **P*<0.0001, ***P*<0.041. Scale bars: 20 μm.

lung morphology and function in Drm1-RKO mice. We therefore investigated the origin of the compensating RBPjκ-positive vSMC population. One possible source is the mesothelium, a specialized epithelium that covers the lung (Herrick and Mutsaers, 2004) in which some RBPjκ-positive cells are detected at E13.5 (gray arrowheads in Fig. 3G-I; supplementary material Fig. S4). The mesothelium can undergo EMT and contribute vSMC to the gut (Wilm et al., 2005) and the heart (Cai et al., 2008; Zhou et al., 2008). To assess mesothelial contribution to lung vSMC, we utilized *Wt1-Cre Rosa*^{EYFP} mice to fate map cells arising from this population (Wilm et al., 2005). Wilm's tumor protein 1 (Wt1) is a mesothelium marker. As seen in the gut, Wt1 expression was restricted to lung mesothelium throughout development (supplementary material Fig. S5A-C), but yellow fluorescent protein (YFP) expression was detected within the lung parenchyma and in endothelial cells three months after birth. YFP-positive cells were also observed in the mural wall, which consists of smooth muscle and pericytes. Importantly, YFP-positive vSMC cells were rarely seen in the lung (supplementary material Fig. S5D-I). Thus, we conclude that the mesothelial lineage does not constitute a major population of vSMC progenitors (see also Que et al., 2008).

Several investigators have reported that endothelial cells can transition into mesenchymal cells, a process called endothelial-mesenchymal transition (EnMT) (Arciniegas et al., 2007). Therefore, we tested whether endothelial cells contribute to pulmonary vSMCs using *Tie1-Cre, R26R* mice (supplementary material Fig. S6). *Tie1-Cre* is exclusively expressed in the endothelium, yet most vSMCs in the proximal pulmonary arteries were double-positive for β-galactosidase and SMA in *Tie1-Cre* mice, confirming that EnMT is responsible for forming most of the early (proximal) vSMCs. The contribution of the *Tie1-Cre* lineage to vSMC gradually declined; at the most distal positions, only an occasional vSMC was β-galactosidase-positive. Distal contribution from EnMT might have continued in Drm1-RKO mice, explaining the presence of RBPjκ-positive vSMC cells in these mice. However, we could not test this hypothesis directly because *Tie1-Cre, Notch1*$^{flox/flox}$ embryos die at E9.5 due to the essential role of Notch1 in vascular development (Conlon et al., 1995; Huppert et al., 2000; Krebs et al., 2000), prior to lung bud formation (supplementary material Fig. S7) (Cheng, 2006).

Lung mesothelial cells contribute to mesenchyme via Notch-triggered EMT

N1IP::CRE^{HI} labeled mesothelial cells (Fig. 1A-F), which prompted us to examine whether Notch signaling regulated EMT in this population. We used the organ culture explant system previously described (Wilm et al., 2005) to address this question. Briefly, we labeled surface mesothelial cells in cultured embryonic lungs at E14.5 with a fluorescent chemical (CCSFE; 5-(and-6)-carboxy-2,7-dichlorofluorescein diacetate succinimidyl ester) for 2 hours (Fig. 5A). Following washout, the lungs were incubated for 48 hours to examine the location of CCSFE-labeled mesothelial cells. Some CCSFE-labeled cells were detected in the mesenchyme at the end of the chase (Fig. 5B), indicating that lung mesothelial cells can undergo EMT ex-vivo. Transforming growth factor β (TGFβ), a general inducer for EMT, increased the number of CCSFE-labeled cells migrating into the mesenchyme, and the TGFRII inhibitor SD208 blocked EMT (Fig. 5C-E). To determine whether Notch signaling participates in EMT and/or mesothelial migration, we repeated the organ culture with embryonic lungs in the presence of the γ-secretase inhibitor DAPT (*N*-[*N*-(3,5-difluorophenacetyl)-L-alanyl]-*S*-phenylglycine *t*-butyl ester). γ-secretase is required for Notch cleavage and therefore for pathway activity. DAPT treatment reduced mesothelial migration in a dose-dependent manner (Fig. 5F-I). Addition of TGFβ restored

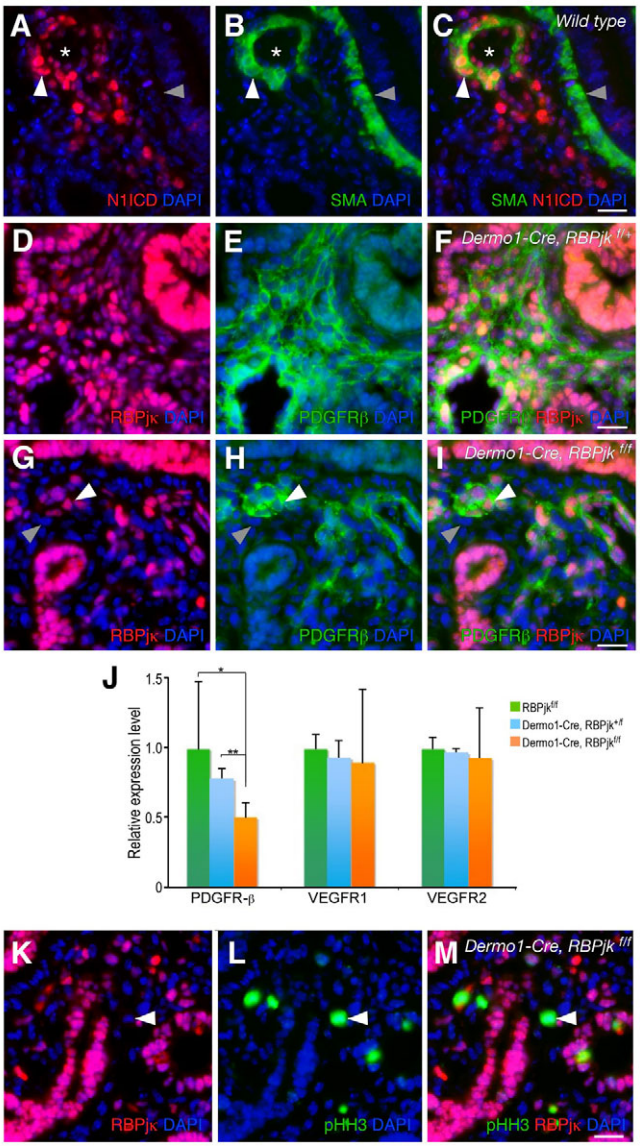

Fig. 4. Notch signaling is functionally activated in developing lung mesenchyme to induce expression of PDGFR-β. (**A-C**) Double staining for N1ICD (red) and SMA (green) illustrates Notch1 activation in endothelial cells (asterisk), vSMCs (white arrowheads) and pericytes, but not bSMC cells (gray arrowheads). Double staining for RBPjκ and PDFGRβ in *Dermo1-Cre, RBPjκ*$^{+/flox}$ (**D-F**) or *Dermo1-Cre, RBPjκ*$^{flox/flox}$ (**G-I**) lungs at E14.5. Cells double-positive for RBPjκ and PDGFR-β are observed in *Dermo1-Cre, RBPjκ*$^{+/flox}$. In *Dermo1-Cre, RBPjκ*$^{flox/flox}$ lung mesenchymal cells, only RBPjκ-positive cells express PDGFR-β (white arrowheads), whereas RBPjκ-negative cells failed (gray arrowheads). Expression levels of PDGFR-β, VEGFR1 and VEGFR 2 were measured with quantitative RT-PCR for E13.5 whole lungs (**J**). Mutants (orange) show significant reduction in expression of PDGFR-β, but not other receptors. Error bars indicate s.d. *P<0.008, **P<0.006. (**K-M**) Double staining for RBPjκ and phospho-histone H3 (pHH3) on E14.5 *Dermo1-Cre, RBPjκ*$^{flox/flox}$ lungs. RBPjκ-negative mesenchymal cells (white arrowheads) were able to enter mitosis, suggesting that Notch signaling is dispensable for maintaining proliferation in the developing lung mesenchyme. Scale bars: 20 μm.

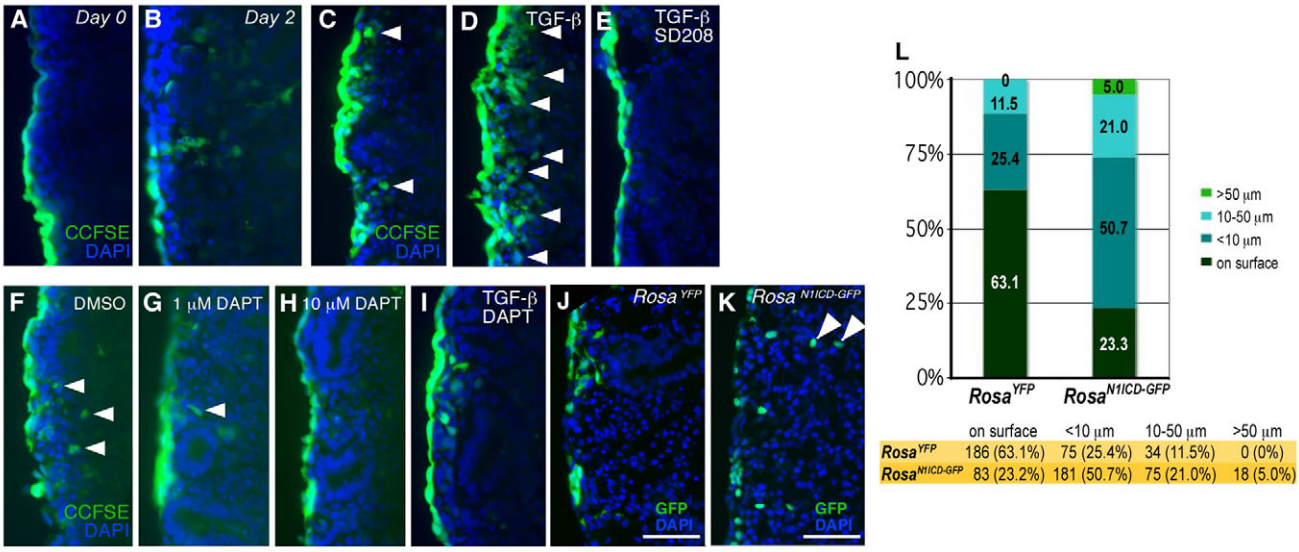

	on surface	<10 μm	10-50 μm	>50 μm
$Rosa^{YFP}$	186 (63.1%)	75 (25.4%)	34 (11.5%)	0 (0%)
$Rosa^{N1ICD-GFP}$	83 (23.2%)	181 (50.7%)	75 (21.0%)	18 (5.0%)

Fig. 5. Notch signaling contributes to mesothelial EMT, and Notch deficiency can be rescued by TGFβ in this process. Lung mesothelium in explants from E14.5 embryos was labeled with CCFSE and visualized on frozen sections using an EGFP filter as indicated. (**A**) At day 0 of culture, only surface cells were positive for CCFSE. (**B**) After two days in culture, some CCFSE-positive cells were observed in the mesenchyme. (**C**,**D**) Culture in 5 ng/ml TGFβ increased the migration of CCFSE-labeled cells (white arrowheads). (**E**) Migration was inhibited by 5 μM SD208, a TGFβ inhibitor. (**F-I**) Culture in DAPT containing medium decreased CCFSE-labeled cells that migrated from the surface in a dose dependent manner (G-H, white arrowheads). TGFβ allowed some migration in the presence of 5 μM DAPT (I). (**J**,**K**) TAT-Cre protein treatment for E14.5 $Rosa^{YFP}$ (J) and $Rosa^{N1ICD-GFP}$ (K) lungs activated the expression of N1ICD-GFP or YFP reporter in mesothelial cells and was followed by in vitro culture for 3 days. Migrated mesothelial cells were detected by staining with anti-GFP antibody on frozen sections. (**L**) The number of migrated mesothelial cells was counted and classified by distance from the surface for each genotype. The number of cells and their percentage in the total population are shown. Scale bars: 50 μm.

migration in the presence of DAPT, indicating that in the presence of strong TGFβ signals, Notch signaling was dispensable for EMT (Fig. 5I).

To confirm that mesothelial EMT could be enhanced by Notch signaling, we locally activated Notch signaling within the lung mesothelial cells in organ culture using a recombinant Cre-recombinase fused to the HIV-TAT peptide (TAT-Cre) (Shaw et al., 2008; Xu et al., 2008). To induce constitutive Notch activity in labeled mesothelial cells, we cultured embryonic lungs from E14.5 $Rosa^{N1ICD-GFP}$ (Murtaugh et al., 2003) or $Rosa^{EYFP}$ mice (in which Cre activity will delete a loxP-flanked stop segment, resulting in expression of N1ICD::GFP or YFP, respectively) with 5 μM TAT-Cre for 5 hours. Following cellar uptake of TAT-Cre on the surface of the lungs and subsequent washout, growth media was replaced and the lung organ cultures were maintained for an additional 3-day period. Mesothelial EMT and migration were assessed by immunohistochemistry with anti-GFP antibody (Fig. 5J-L). Whereas 37% of mesothelial cells underwent EMT in control *ROSA-YFP* cultures, 77% of cells expressing N1ICD::GFP underwent EMT. Furthermore, 5% of the N1ICD cells migrated more than 50 μm inwards, whereas control YFP^{+} cells were never detected that deep (white arrowheads in Fig. 5K,L). These results indicate that Notch activation is sufficient to induce EMT in the mesothelium and that it accelerated the mobility of mesothelium-derived cells.

Clara cells experience Notch1 activation during lung epithelial development

By P21, when lung epithelial development is nearly complete, all of the lineages derived from cells experiencing Notch1 activation (as marked by *N1IP::CRE*^{HI}, *R26R*) have been marked. Histological analysis of intact lungs identified β-galactosidase-positive cells as airway epithelial cells (Fig. 6A,B). Immunohistochemistry for CC10 (Clara cells; Fig. 6C), acetylated tubulin (ciliated cells; Fig. 6D), and calcitonin gene related peptide (CGRP) (PNECs; Fig. 6E) determined that β-galactosidase-positive cells differentiated predominately into Clara cells. A few ciliated cells were also labeled (see below). To obtain a three-dimensional (3D) image of how the epithelial lineages were distributed in the bronchial tree, we manually removed alveolar capillary cells that are robustly labeled with β-galactosidase, obscuring the epithelium. β-galactosidase-positive cells appeared throughout the conducting airway (Fig. 6F), reaching the highest density in the distal conducting airways (Fig. 6G-I).

To examine the role of Notch signaling in lung epithelia, we generated *SHH-Cre, RBPjκ*$^{flox/flox}$ (Shh-RKO) mice (Harfe et al., 2004; Harris et al., 2006). Staining for RBPjκ in developing Shh-RKO lungs confirmed that RBPjκ was absent from lung epithelial cells but its expression remained intact in all other pulmonary lineages (supplementary material Fig. S8A-D). Unlike Pfout1-deficient mice that survive to weaning (Tsao et al., 2009), Shh-RKO mutant mice die at birth from an undetermined cause, apparently unrelated to the lung because breathing appeared normal, mice were not cyanotic and no morphological pulmonary defects were observed. Shh-RKO reproduced the phenotypes seen with loss of Pofut1 (Tsao et al., 2009), namely, expansion of Foxj1-positive ciliated cells at the expense of Clara cells throughout the entire lung epithelium (supplementary material Fig. S8I-O). The stem cell population still gave rise to normal alveolar epithelial cell types (Type II and Type I cells) in Shh-RKO lungs, indicating that the defect was restricted to the Clara and ciliated lineages (supplementary material Fig. S8P-S). Collectively, these data

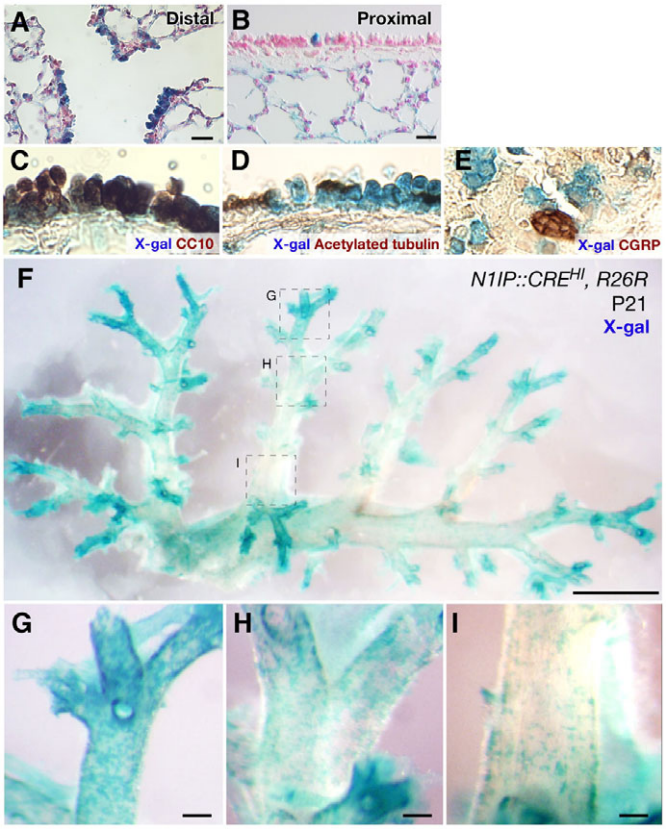

Fig. 6. Cells experiencing Notch1 activation become Clara and ciliated cells, but not PNECs. The fate of cells experiencing Notch activation was visualized using X-gal staining in *N1IP::CRE^{HI}, R26R* lungs at P21. β-galactosidase-positive epithelial cells (**A-E**) were identified by double staining for β-galactosidase and CC10 (**C**), acetylated tubulin (**D**) or CGRP (**E**). The Notch-experienced cells contributed to Clara and some ciliated cells but not PNECs. (**F**) X-gal staining for whole lungs revealed gradual distribution from low (proximal, B) to high (distal, A) density of β-galactosidase-labeled cells in conducting airways. (**G-I**) Areas indicated by dashed squares in F are magnified in G-I. Scale bars: A,B, 20 μm; F, 1 mm; G-I, 100 μm.

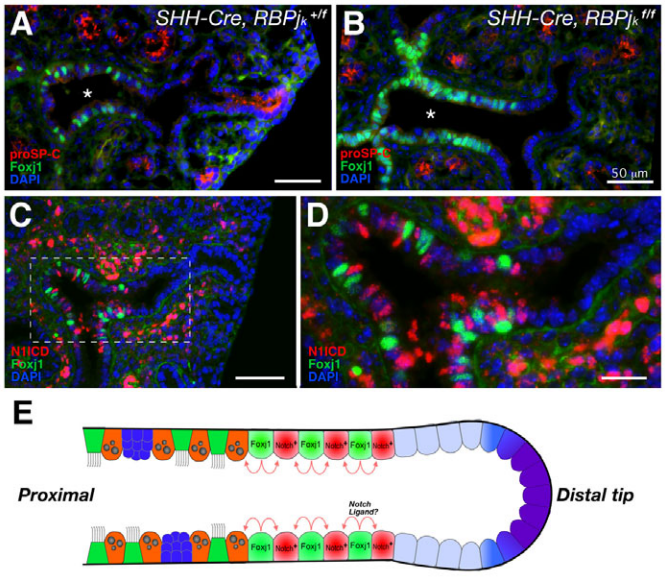

Fig. 7. Clara and ciliated cell fates are delineated from bi-potential progenitors through a lateral inhibition mechanism related to Notch signaling. (**A**,**B**) Immunofluorescence of E16.5 distal tip to proximal epithelial cells stained with anti-proSP-C (distal bud marker, red) and anti-Foxj1 (a ciliated cell marker, green) revealed that early ciliated cells distribute in a 'salt-and-pepper' fashion in the proximal epithelium of control lungs (A, asterisk). In RBPjκ-deficient epithelium, nearly all proximal epithelial cells were Foxj1-positive (B, asterisk). (**C**,**D**) Double staining for N1ICD (red) and Foxj1 (green) demonstrates Notch1 activation in cells adjacent to Foxj1-positive cells. Dotted square in C indicates area magnified in D. (**E**) Model of the role of Notch signaling in the determination of Clara or ciliated cell fate. At the pseudoglandular stage, the elongating distal tip includes epithelial stem cells (purple). A subset of progenitor cells initiate Foxj1 expression (green) as they differentiate into ciliated cells. Foxj1-positive cells might activate Notch signaling in neighboring cells (as marked by N1ICD, red) to suppress the ciliated fate and promote Clara cell differentiation. Finally, the conducting airways generate Clara (orange), ciliated cells (green trapezoid) and PNECs (blue) in the proximal airways. Scale bars: A-C, 50 μm; D, 25 μm.

suggest that Notch signaling functions during lung development in a bi-potential progenitor to either induce the Clara cell fate or to permit Clara cell differentiation by blocking a default ciliated fate. To differentiate between these possibilities, we examined ciliated cell production during the pseudoglandular stage, when ciliated cells and Clara cells are determined from an epithelial progenitor cell population residing at the branch tip among proSP-C-positive cells (Fig. 7A). At E16.5, Foxj1 (which marks ciliated cells) was observed only within the proximal airway in a 'salt and pepper' pattern (Fig. 7A, asterisk), suggesting that determination of ciliated cell fate occurs in a transitional zone located between distal stem cells and proximal differentiated daughters. By contrast, nearly all the proximal cells expressed Foxj1 in *RBPjκ*-deficient epithelium (Fig. 7B, asterisk). The salt and pepper distribution of Clara and ciliated cells further suggests a lateral inhibition mechanism involving activation of Notch signaling in neighbors of nascent ciliated cells at the transition zone (Fig. 7E). To test whether lateral interaction among decedents led to Notch1 activation, we used an anti-N1ICD antibody to detect activated Notch1. Double staining for N1ICD and Foxj1 at E16.5 revealed a mutually exclusive distribution of these markers (Fig. 7C,D). Coupled with N1IP::Cre labeling (Fig. 6), these data indicate that neighbors of Foxj1-positive cells, but not the distal progenitors, activate Notch signaling. Cells experiencing Notch1 activation become Clara cells. The few β-galactosidase-positive ciliated cells we saw were either derived from a labeled Clara cell (Perl et al., 2002) or indicate that Notch signaling is activated again during formation of a ciliated cell from a Clara cell.

To test whether ciliated cells required canonical Notch signaling subsequent to their formation, we generated *FOXJ1-Cre, RBPjκ$^{flox/flox}$* mutant mice in which RBPjκ was deleted after the ciliated fate was determined. These mice were viable and fertile and displayed no change in the frequency of ciliated or Clara cells (supplementary material Fig. S9). Examination of *SP-C-rtTA, (tetO)$_7$-Cre, Rosa$^{N1ICD-GFP}$* triple transgenic mice revealed a reduction in ciliated cells, establishing that N1ICD inhibits ciliated cell fate acquisition [data not shown and Guseh et al. (Guseh et al., 2009)]. These observations expand the data reported earlier (Tsao et al., 2009) and confirm that Pofut1 deletion expanded the ciliated epithelium by eliminating Notch1 signals.

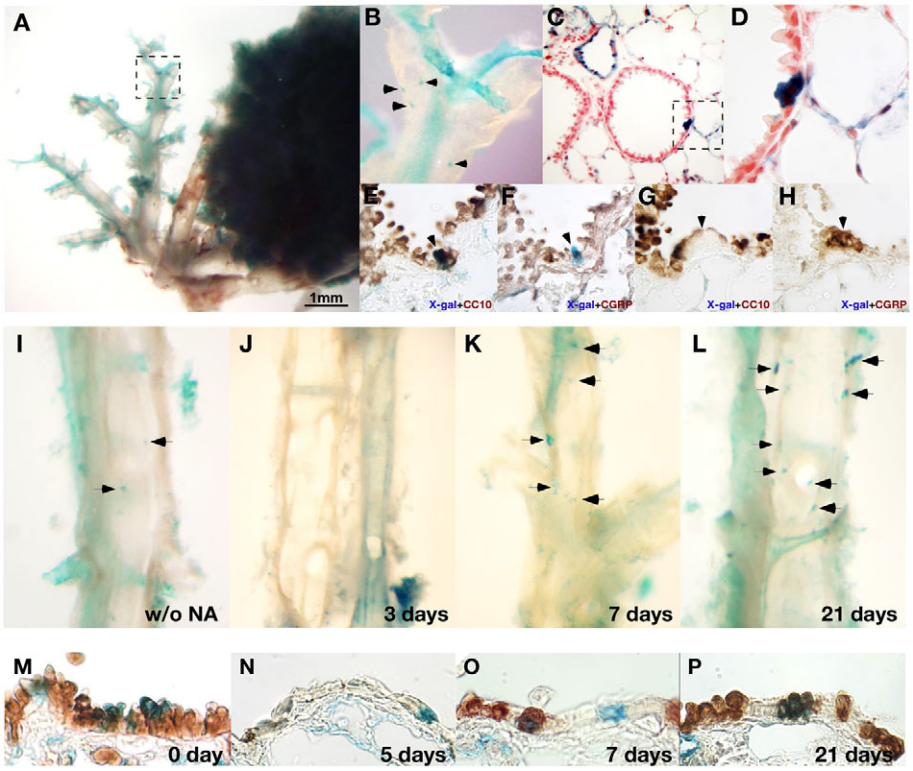

Fig. 8. Notch1 signaling is involved in Clara cell regeneration in the adult lung following injury. The fate of cells that experienced Notch1 activation was visualized in *N1IP::CRE^{LOW}, R26R* lungs at P14. X-gal staining for whole lungs (**A**,**B**) and lung sections (**C**,**D**) revealed mosaic β-galactosidase activity in the epithelium (B-D, black arrowheads). CC10 (**E**,**G**) or CGRP (**F**,**H**) staining on neighboring X-gal-stained sections identified β-galactosidase-positive Clara cells but not PNECs. To induce airway injury and regeneration, conducting airways of *N1IP::CRE^{LOW}, R26R* mice were injected with a single dose of naphthalene. At 3 days after injection, all β-galactosidase-positive cells had disappeared (**I**,**J**). Subsequently, labeled cells increased in number, forming small clusters (**K**,**L**). CC10 staining revealed that Notch1 activation occurred in regenerating epithelia before differentiation into Clara cells (**M-P**), suggesting that Notch1 signaling is involved in the terminal differentiation into Clara cells rather than the maintenance of the stem cell and/or progenitor population for lung epithelial cells.

Notch signaling has a role in Clara cell regeneration but not maintenance in the adult lung

To determine whether Notch1 was reactivated during Clara cell regeneration, we used *N1IP::CRE^{LOW}, R26R* mice (Vooijs et al., 2007) that label Clara cells infrequently compared to *N1IP::CRE^{HI}* (compare Fig. 8A,B and Fig. 6F,G). A few β-galactosidase-positive cell clusters could be discerned within the conducting airway epithelia at P14 (Fig. 8A,B). Histological analysis revealed that each cluster included one to eight cells (Fig. 8C,D), and that these cells were positive for CC10 (Clara cell marker) but negative for CGRP (PNEC marker). Next, we injured the airway epithelium in *N1IP::CRE^{LOW}, R26R* mice with a single injection of naphthalene and examined β-galactosidase staining patterns throughout the regeneration process. Naphthalene toxicity induced apoptotic death of most Clara cells within conducting airways by 3 days. Following this, lung epithelial stem cells initiate a regeneration program, which is nearly complete 14 days after a single exposure to naphthalene (Plopper et al., 1992; Rawlins et al., 2007). Following injury, all epithelial β-galactosidase-positive cells disappeared (Fig. 8J), and regeneration was initiated from β-galactosidase-negative cells. β-galactosidase-positive cells began to reappear 5 days post-injury (Fig. 8N) and increased in number within clusters as the epithelium recovered (Fig. 8K,L). Furthermore, as judged by the timing of β-galactosidase and CC10 expression at 5, 7 and 21 days post-injury, Notch1 activation preceded Clara cell differentiation during regeneration (Fig. 8M-P, Table 1).

To test whether Clara cells required Notch for their maintenance, we generated triple-transgenic *CCSP-rtTA, (tetO)$_7$-Cre, RBPjκ$^{flox/flox}$* mice. Although some lung toxicity and mosaicism was reported in these mice (Sisson et al., 2006), mosaic deletion patterns of RBPjκ would predict that no RBPjκ$^{-/-}$ Clara cells would be found 6 weeks after doxycycline (DOX) administration if RBPjκ played an important role in Clara cell maintenance. When DOX was added to the diet beginning at P31, many *RBPjκ*-null Clara cells were detected by double staining (supplementary material Fig. S10) indicating that they were not replaced by cells expressing RBPjκ. Collectively, these results demonstrate that Notch1 activation did not mark stem cells or their transient-amplifying daughters. Instead, it was activated in cells during the final stages of differentiation, where it might regulate mucous production [data not shown and Guseh et al. (Guseh et al., 2009)]. Notch signaling might not be required for Clara cell differentiation or maintenance, but this conclusion is confounded by the low turnover rates of the adult lung.

PNEC fate restriction by Hes1 is largely independent of canonical Notch signals

A role for Notch upstream of Hes1 in regulating PNEC fate selection has been proposed (Ito et al., 2000). Pofut1-deficient mice appear

Table 1. Frequency of a β-galactosidase and CC10 double-positive epithelial cell in regenerative *N1IP::CRE, R26R* lung after naphthalene injection

	0 days	5 days	7 days	21 days
β-gal$^+$, CC10$^+$	183	6	78	260
Total β-gal$^+$	192	81	231	326
Section/sample	9/3	6/2	10/3	10/3
	95.3%	7.4%	59.2%	79.8%

Data represent the number of β-galactosidase-positive (β-gal$^+$) or β-galactosidase and CC10 double-positive cells in *N1IP::CRE, R26R* lung epithelium during the regenerative process. The total number of sections examined and the percentage of double-positive cells of the total β-gal$^+$ cell population is shown. Although less than 8% of β-gal$^+$ cells were double-positive at 5 days after injury, the percentage increased to about 80% at 21 days.

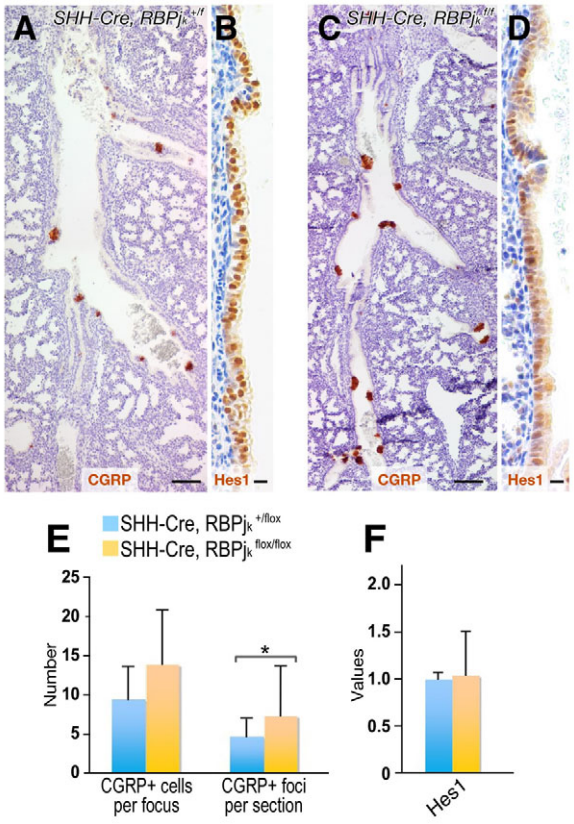

Fig. 9. Disruption of Notch signaling does not significantly change PNEC specification or *Hes1* expression. Immunostaining for CGRP (**A**,**C**) and Hes1 (**B**,**D**) in E18.5 *SHH-Cre, RBPjκ*$^{+/flox}$ control (A,B) and *SHH-Cre, RBPjκ*$^{flox/flox}$ mutant (B,D) lungs. (**E**) RBPjκ ablation in developing epithelium (orange) minimally increased the number of CGRP-positive cells per focus, and of CGRP-positive foci per section, compared to controls (blue), but this difference was not statistically significant. Counts represent average cell number per foci from six sections in each group. (**F**) Quantitative RT-PCR analysis revealed no alteration in *Hes1* mRNA expression in the RBPjκ-deficient epithelium compared to controls. Error bars indicate s.d. **P*<0.01. Scale bars: A,C, 50 μm; B,D, 10 μm

to confirm this suggestion because they contain an increased number of PNECs (Tsao et al., 2009). We thus examined the distribution of PNECs in Shh-RKO mice within the lung epithelia using immunohistochemistry. Although the average number and size of PNEC clusters was slightly increased in *RBPjκ*-deficient epithelia (Fig. 9A,C,E), this increase was similar to the increase reported in *Hes1* heterozygote lungs (Ito et al., 2000). Whereas Hes1 expression was essentially abolished in the epithelia of *Pofut1*-deficient lungs (Tsao et al., 2009), Hes1 in *RBPjκ*-deficient epithelia was not dramatically reduced at either the protein or mRNA levels as late as E18.5 (Fig. 9B,D,F). Thus, Hes1 expression in lung epithelial cells does not rely on canonical Notch signaling.

Discussion

In this study, we used genetic analyses to decipher where Notch signaling acts during lung development. In addition, the new *N1IP*^{HI}*::CRE, R26R* mice permitted a higher resolution mapping of the lineages experiencing at least one round of Notch1 activation. Conditional gene targeting was complemented by organ culture experiments to confirm the role of activated Notch1. With these tools, we report a function for Notch signaling in vSMC specification and in regulating mesothelial EMT and migration rates, and confirm recent observations describing Notch signaling as a suppresser of ciliated cell fate that permits or induces secretory cell formation (Guseh et al., 2009; Tsao et al., 2009). We extend these observations by providing evidence for direct Notch1 involvement in this process. Notch activation in regenerating Clara cells could reflect regulation of mucous secretion (Guseh et al., 2009). Finally, we report interesting differences between mice lacking *RBPjκ* and *Pofut1* (longevity, role in *Hes1* expression) and report a function for Notch signaling after EMT occurred in the heart. This might reflect an impact of *Pofut1* on lung development via non-canonical Notch activity or additional substrates. However, *RBPjκ* is dedicated to canonical Notch signaling in the lung, where RBPjκ-like protein (RBPL) will compensate for Notch-independent RBPjκ activity such as interaction with Pitf1a (Beres et al., 2006).

Vascular, but not bronchial, SMC development requires Notch signaling

Ablation of Notch signaling in lung mesenchyme and mesothelium with the *Dermo1-Cre* transgene resulted in no obvious morphological alterations. Published reports (Proweller et al., 2007) established that canonical Notch signaling was not required for the maintenance of the SMC cell fates; indeed, bSMC formed in the absence of *RBPjκ* as efficiently as they did in its presence. By contrast, selection of the vSMC fate, or migration of SMCs arising outside of the arteries, was severely impaired. vSMC were strongly labeled in *N1IP::CRE*^{HI}, *R26R* mice, implying that in addition to its established role in promoting endothelial cell differentiation into a vascular network (Gridley, 2007), Notch1 activation was required within vSMC precursors. A possible explanation for the involvement of Notch in arterial vSMC differentiation has been proposed based on observations that three SMC marker genes (SM-MHC, SMA and PDGFR-β) responded to Notch activation (Doi et al., 2006; Jin et al., 2008; Noseda et al., 2006). We find that expression of PDGFR-β is significantly reduced in RBPjκ-deficient cells, confirming that Notch signaling is required cell-autonomously for PDGFR-β expression (Jin et al., 2008). Because PDGF signaling plays a crucial role in the recruitment of pericytes and vSMC progenitors during vasculogenesis (Andrae et al., 2008), loss of RBPjκ (and hence, PDGFR-β) might impair vSMC recruitment. *Jagged1*-expressing peripheral endothelial cells activate Notch signaling on pericytes, promoting SMC differentiation (High et al., 2008; Liu et al., 2009). Therefore, Notch signaling is required both for recruitment and differentiation in vSMC. Accordingly, we detected cells that experienced Notch1 activation in mesenchymal cells surrounding the lung vasculature. Bronchial SMC differentiation depends on FGF10 (Mailleux et al., 2005). Therefore, Notch and FGF10 might separate vascular and bronchial SMC progenitors, respectively, from mesenchymal stem cells. Importantly, in the absence of RBPjκ in vivo, vSMCs still formed outside the Dermo1-Cre lineage, presumably to compensate for the loss of Notch signaling, obscuring a potential phenotype observed with GSI or antisense oligonucleotides in organ culture.

Notch and TGFβ signaling promote EMT in lung mesothelium

Because *Dermo1-Cre* is active in the mesenchyme and in the mesothelium, and transdifferentiation of mesothelial cells via EMT was described in the heart (Cai et al., 2008; Wada et al., 2003; Zhou et al., 2008), the gut (Wilm et al., 2005) and the liver (Ijpenberg et

al., 2007), we used *Wt1-Cre, R26YFP* mice to determine whether vSMC were derived, in a Notch dependent manner, from the mesothelium. Although YFP-positive cells were observed in vascular endothelium and the mural wall, we concluded that the mesothelial lineage (Wt1, Dermo1-positive) did not contribute significantly to the vSMC population under normal conditions (see also Que et al., 2008). Vital dye pulse-chase experiments, constitutive Notch1 activation, and inhibitor studies in lung organ cultures identified a role for Notch signaling alongside TGFβ in mesothelial EMT. Thus, if mesothelial cells were involved in vSMC rescue, in vitro inhibition of Notch signaling would greatly reduce their ability to rescue. In addition, Notch activation enhanced migration of mesothelium-derived cells; this finding might have important implications for understanding the aggressive metastatic nature of malignant mesothelioma because elevated Notch signaling has been observed in malignant human mesothelial cells (Graziani et al., 2008).

Notch signaling is essential for endothelial development

Another potential source for vSMCs in *Dermo1-Cre, RBPjκ$^{flox/flox}$* mice is endothelial cells, which remained positive for Notch signaling and have been known to undergo EnMT in the lung (Arciniegas et al., 2007). However, due to the early lethality associated with endothelial-specific loss of *Notch1*, we could not demonstrate a contribution of EnMT to vSMC in *Dermo1-Cre, Tie1-Cre, RBPjκ$^{flox/flox}$* animals. The origin of the rescuing cells, therefore, remains speculative, awaiting creation of an endothelial-specific *Flp*-recombinase-based reporter. Importantly, Notch signaling is necessary to promote endocardial EnMT during formation of cardiac valves (Timmerman et al., 2004), and activation of Notch signaling is sufficient to induce EnMT in vitro (Noseda et al., 2004).

On the basis of our experiments, we can thus propose a speculative model explaining how GSI and Notch1 antisense oligonucleotides impact branching morphogenesis, yet two genetic models of global Notch loss [this study and Tsao et al. (Tsao et al., 2009)] did not reproduce the branching phenotype. Endothelial cells deficient in Notch signaling display branching and tube formation defects (Gridley, 2007; Hellstrom et al., 2007). In our opinion, the profound effects of GSI and antisense nucleotides on development and branching of lung anlagen growing in organ culture can thus be attributed to the disruption of vascular network formation, failed recruitment of vSMC, failed compensation by EnMT, or some combination of these. Indeed, DAPT-treated Tie2-GFP lung rudiment cultures show extensive migration and deficient vasculogenesis, whereas airway branching continues at an enhanced rate (Robert Mecham, Washington University, St Louis, MO, personal communication). We conclude that the negative effects of global Notch inhibition are most probably a reflection of losing the vascular endothelial network and/or its associated SMCs, which must therefore negatively regulate branching morphogenesis and positively contribute to maintaining distal fates.

The primary function of Notch signaling in lung epithelial cells is in permitting selection of Clara cell fate

Guseh and colleagues have reported that misexpression of a constitutively active Notch1 fragment with a mosaic *SPC-Cre* transgene causes mucous metaplasia of the airway and decreases the number of ciliated cells. In addition, this non-physiological and persistent activation generated alveolar cysts (Guseh et al., 2009). They interpreted this to suggest that Notch signaling suppresses alveolar development. In contrast to these observations, loss-of-function analysis of RBPjκ, a core component of canonical Notch signaling (this study), or Pofut1 (Tsao et al., 2009), which might be required for both canonical and non-canonical functions, did not support a role for physiological Notch signing within lung epithelial cells in regulating alveolar morphogenesis [(Morimoto and Kopan, 2009; Tsao et al., 2009) and data not shown]. *RBPjκ*- or *Pofut1*-null epithelium did not display alterations in branching morphology and contained normal alveoli. We concur with the conclusion that loss of Notch signaling leads to loss of Clara cells and provide evidence that Notch1 is involved. We describe a distal-to-proximal transition zone in which ciliated cells induce Notch activation in their neighbors, inhibiting them from selecting the same fate and permitting development of Clara cells. Finally, tracing the lineage of cells experiencing Notch1 activation indicates that these cells overwhelmingly assume the Clara cell fate (with a few ciliated cells labeled secondarily). Interestingly, Notch1 was activated again during epithelial regeneration following pharmacological injury. Notably, Notch1 activation was not involved in maintenance of the epithelial stem cells. Several previous reports show that Wnt signaling promotes proliferation of the airway epithelial stem cells early during regeneration (Reynolds et al., 2008; Zhang et al., 2008). Induction of Notch ligand by Wnt activity (Estrach et al., 2006) might trigger Notch activation during Clara cell regeneration.

Notch signaling was reported previously to be involved in a similar lateral inhibitory process, in which ciliated cells inhibit their neighbors from assuming the same fate. In the zebrafish pronephros, transporting epithelia and multiciliated cells (MCCs) form in a salt and pepper pattern (Liu et al., 2007). It has been shown that zebrafish Jagged2 expression in presumptive MCCs induced activation of zebrafish Notch3 in neighboring cells, blocking MCC fate and driving the alternative transporting epithelial cell fate. In addition, a Hes1-related protein was involved (Ma et al., 2007). In *Xenopus*, ciliated cells express Delta ligands to activate Notch signaling (and Hes-related proteins), inhibiting the selection of ciliated cells by neighboring epidermal cells (Deblandre et al., 1999).

Deletion of Hes1 and Pofut impacts PNEC differently to loss of RBPjκ

Although *Hes1* is a well-characterized Notch target gene in some cells, it can be regulated by other pathways (Nakayama et al., 2008; Yoshiura et al., 2007). Accordingly, it has been reported that *Hes1* and *Pofut1* regulate PNEC foci number as well as size (Ito et al., 2000; Tsao et al., 2009), yet *RBPjκ*-deficient mice retain *Hes1* expression, and the number of PNECs was decreased only to the intermediate degree seen in *Hes1* heterozygotes, not nulls. These data suggests that *Hes1* expression might be controlled by upstream signals to which Pofut1 (but not RBPjκ) contributes. This could either imply involvement of other pathways (Nakayama et al., 2008; Yoshiura et al., 2007) or non-canonical Notch signaling.

Materials and Methods

Whole-mount X-gal staining

To visualize N1IP-CRE activity, the tracheas of 2- to 3-week-old N1IP-CRE, R26R mice were filled with 0.2% GAD fixative (0.2% glutaraldehyde, 2 mM $MgCl_2$ in PBS) before isolation. After removal of the lungs from the thorax, both were further fixed in 0.2% GAD fixative for 1 hour at room temperature. The fixed lungs were washed (in 2 mM $MgCl_2$, 0.1% Tween-20, 0.05% dextrin in PBS) three times for 5 minutes. After washing, lungs were filled with X-gal solution (2 mM $MgCl_2$, 35 mM potassium ferrocyanide, 35 mM potassium ferricyanide, 1 mg/ml X-gal, 0.02% NP-40, 0.01% Na deoxycholate in PBS). The X-gal-filled lungs were submerged in X-gal solution and incubated for 12-24 hours at 4°C in the dark, then post-fixed with 4% paraformaldehyde overnight at 4°C.

X-gal staining of tissue sections

β-galactosidase-expressing fetal lungs were dissected in ice-cold PBS, then fixed with 0.5% GAD fixative (0.5% glutaraldehyde, 2 mM $MgCl_2$, 0.1% Tween-20 in PBS) for 1 hour at 4°C. The fixed lungs were washed in solution three times for 5 minutes each before equilibration with 30% sucrose in PBS. After embedding in OCT compound (Sakura), frozen sections (5-6 mm) were generated and either stored at –20°C or incubated in X-gal solution for 3-6 hours at 37°C. The stained sections were counterstained with Nuclear Fast Red (Vector Laboratory).

Immunohistochemistry

Fetal lungs were dissected and fixed in 4% paraformaldehyde for 1 hour to overnight at 4°C, embedded in paraffin or OCT (for frozen sections) and sectioned at 6-7 μm. 4% formaldehyde was used for the detection of β-galactosidase. Sections were rehydrated and treated with 0.3% hydrogen peroxide in MeOH for 10 minutes before staining. The antibodies and conditions used for individual immunohistochemical analyses are described in supplementary material Table S1.

Lung organ culture

E14.5 lungs were collected from timed pregnant CD1 wild-type or *N1IP::CRE, R26R* mice and labeled with 40 μM CCFSE (5-(and-6)-carboxy-2,7-dichlorofluorescein diacetate, succinimidyl ester; Molecular Probes) in DMEM containing 10% FBS, 1 mM L-glutamine and 1 mM penicillin-streptomycin for 2 hours at 37°C, 5% CO_2. The CCFSE was prepared as a 20 mM stock solution in DMSO. In some experiments, samples were treated with 5 μM recombinant Tat-Cre protein for 5 hours at 37°C, 5% CO_2. Subsequently, the labeled lungs were washed and cultured on a filter (cell culture insert, 1.0 μm pore size P.E.T. track-etched membrane; Falcon) in medium without CCFSE or Tat-Cre for 48 hours at 37°C, 5% CO_2. TGFβ (2 μg/ml; R&D Systems), SD208 (5 mM; Calbiochem) or DAPT (1 mM; Calbiochem) was added to culture medium to appropriate final concentrations (described in each figure legend). To prepare frozen blocks, at least three whole lungs at end time points were fixed using fresh 4% formaldehyde for 1 hour at 4°C followed by equilibration with 30% sucrose in PBS. Sections (6 μm) were cut and mounted with Vectamount with DAPI (Vector Laboratories) or stained with anti-GFP-antibody (see supplementary material Table S1) for Tat-Cre experiments. Using a Carl Zeiss Axio imager Z1 microscope, the fluorescence of CCFSE was observed with the EGFP filter under 400× magnification. To quantify mesothelial EMT, ten photographs of GFP-positive cells were taken for each genotype under 400× view.

Recombinant TAT-Cre protein

TAT-Cre recombinant protein was expressed and purified according to previously described protocols (Peitz et al., 2002). Briefly, *Escherichia coli* TUNER(DE3)p*Lac*I (Novagen) containing pTriEx(Novagen)-His-TAT-NLS-Cre was cultured with LB medium containing 100 mg/ml ampicillin and 34 mg/ml chloramphenicol at 37°C with shaking until the OD_{600} was 0.9-1.0. Expression was induced with 0.5 mM isopropylthiogalactoside for 4 hours. Cells were harvested, resuspended in phosphate buffer (50 mM Na_2HPO_4, 5 mM Tris pH 7.8, 500 mM NaCl) containing lysozyme (Sigma) and Benzonase (Novagen) for lysis. TAT-Cre protein was purified from the supernatant with Ni-NTA matrix (Qiagen). The matrix was washed extensively with phosphate buffer containing 20 mM imidizole and eluted with phosphate buffer containing 250 mM imidazole. Protein-containing fractions were pooled and dialyzed against 600 mM NaCl, 20 mM HEPES, and subsequently against 600 mM NaCl, 20 mM HEPES, 50% glycerol to concentrate.

Mouse strains

RBPjκ$^{flox/flox}$ mice were kindly provided by Tasuku Honjo, Kyoto University, Kyoto, Japan (Tanigaki et al., 2002). Dermo1-Cre mice were generated by David Ornitz at Washington University, St Louis, MO (Yu et al., 2003). *FOXJ1-Cre* mice were a kind gift from Michael Holtzman, Washington University, St Louis, MO (Zhang et al., 2007). These mice were maintained on the CD1 background. Dermo1-Cre mice were mated to *RBPjκ*$^{flox/flox}$ mice to generate heterozygous *Dermo1-Cre*, *RBPjκ*$^{+/flox}$ mice, which were then crossed to *RBPjκ*$^{flox/flox}$ mice to create *Dermo1-Cre*, *RBPjκ*$^{flox/flox}$ conditional knockout animals. *FOXJ1-Cre, RBPjκ*$^{flox/flox}$ mice were generated in the same way.

The *N1IP::CRE* (Vooijs et al., 2007), *Wt1-Cre* (Wilm et al., 2005) and *CCSP-rtTA, (Tet)7O-Cre* (Perl et al., 2002) mice were described previously. *SHH-Cre* is commercially available at The Jackson Laboratory. All animal procedures were performed according to NIH guidelines and maintained in the animal facility under Washington University animal care regulations.

RNA isolation, cDNA synthesis, and qRT-PCR analysis

Embryonic lung mRNA was isolated using the RNeasy kit (Qiagen) following the manufacturer's instructions. cDNA was synthesized using the SuperScript II first-strand cDNA synthesis kit (Invitrogen). Quantitative RT-PCR was performed on an ABI 7500 machine using Power SYBR Green for Foxj1, CC10, Hes1 and Gapdh. Amplification and analyses were performed according to the manufacturer's instructions. All reactions were normalized to Gapdh. Results were plotted as relative expression compared with control, where control was scaled to 1.

The authors thank Adrian Shifren, David Ornitz, Rober Mecham and Scott Boyle (from Washington University, St Louis, MO) for careful reading of the manuscript. We also thank David Ornitz for the Dermo1-Cre mice, Tasuku Honjo for the conditional *RBPjκ*$^{flox/flox}$ mice and Steven Brody for anti-FoxJ1 antibody. This work was supported by Washington University and by NIH grants P50 CA094056 (David Piwnica-Worms) and RO1 DK066408 (R.K.). M.M. was supported by a Toyobo Biotechnology Foundation Long-term Research Grant, the Japanese Society for the Promotion of Science and The Kanae Foundation for the Promotion of Medical Science. We wish to thank Patricia Gonzalez-DeWhitt (Eli Lilly and Company, Indianapolis, IN) for the generous gift of the rabbit anti-VLLS antibody. Deposited in PMC for release after 12 months.

Supplementary material available online at
http://jcs.biologists.org/cgi/content/full/123/2/213/DC1

References

Andrae, J., Gallini, R. and Betsholtz, C. (2008). Role of platelet-derived growth factors in physiology and medicine. *Genes Dev.* **22**, 1276-1312.

Arciniegas, E., Frid, M. G., Douglas, I. S. and Stenmark, K. R. (2007). Perspectives on endothelial-to-mesenchymal transition: potential contribution to vascular remodeling in chronic pulmonary hypertension. *Am. J. Physiol. Lung Cell Mol. Physiol.* **293**, L1-L8.

Beres, T. M., Masui, T., Swift, G. H., Shi, L., Henke, R. M. and MacDonald, R. J. (2006). PTF1 is an organ-specific and Notch-independent basic helix-loop-helix complex containing the mammalian Suppressor of Hairless (RBP-J) or its paralogue, RBP-L. *Mol. Cell. Biol.* **26**, 117-130.

Cai, C. L., Martin, J. C., Sun, Y., Cui, L., Wang, L., Ouyang, K., Yang, L., Bu, L., Liang, X., Zhang, X. et al. (2008). A myocardial lineage derives from Tbx18 epicardial cells. *Nature* **454**, 104-108.

Cardoso, W. V. and Lu, J. (2006). Regulation of early lung morphogenesis: questions, facts and controversies. *Development* **133**, 1611-1624.

Cheng, H. (2006). The role of Notch1 and Notch2 in mammalian kidney and cardiovascular development. In *Molecular Biology and Pharmacology*, vol. MD, pp. 114. St Louis: Washington University.

Conlon, R. A., Reaume, A. G. and Rossant, J. (1995). Notch1 is required for the coordinate segmentation of somites. *Development* **121**, 1533-1545.

Deblandre, G. A., Wettstein, D. A., Koyano-Nakagawa, N. and Kintner, C. (1999). A two-step mechanism generates the spacing pattern of the ciliated cells in the skin of Xenopus embryos. *Development* **126**, 4715-4728.

Doi, H., Iso, T., Sato, H., Yamazaki, M., Matsui, H., Tanaka, T., Manabe, I., Arai, M., Nagai, R. and Kurabayashi, M. (2006). Jagged1-selective notch signaling induces smooth muscle differentiation via a RBP-Jkappa-dependent pathway. *J. Biol. Chem.* **281**, 28555-28564.

Estrach, S., Ambler, C. A., Celso, C. L. L., Hozumi, K. and Watt, F. M. (2006). Jagged 1 is a beta-catenin target gene required for ectopic hair follicle formation in adult epidermis. *Development* **133**, 4427-4438.

Galambos, C. and Demello, D. (2007). Molecular mechanisms of pulmonary vascular development. *Pediatr. Dev. Pathol.* **10**, 1-17.

Graziani, I., Eliasz, S., De Marco, M. A., Chen, Y., Pass, H. I., De May, R. M., Strack, P. R., Miele, L. and Bocchetta, M. (2008). Opposite effects of Notch-1 and Notch-2 on mesothelioma cell survival under hypoxia are exerted through the Akt pathway. *Cancer Res.* **68**, 9678-9685.

Gridley, T. (2007). Notch signaling in vascular development and physiology. *Development.* **15**, 2709-2718.

Guseh, J. S., Bores, S. A., Stanger, B. Z., Zhou, Q., Anderson, W. J., Melton, D. A. and Rajagopal, J. (2009). Notch signaling promotes airway mucous metaplasia and inhibits alveolar development. *Development* **136**, 1751-1759.

Hall, S. M., Hislop, A. A., Pierce, C. M. and Haworth, S. G. (2000). Prenatal origins of human intrapulmonary arteries: formation and smooth muscle maturation. *Am. J. Respir. Cell Mol. Biol.* **23**, 194-203.

Harfe, B. D., Scherz, P. J., Nissim, S., Tian, H., McMahon, A. P. and Tabin, C. J. (2004). Evidence for an expansion-based temporal Shh gradient in specifying vertebrate digit identities. *Cell* **118**, 517-528.

Harris, K. S., Zhang, Z., McManus, M. T., Harfe, B. D. and Sun, X. (2006). Dicer function is essential for lung epithelium morphogenesis. *Proc. Natl. Acad. Sci. USA* **103**, 2208-2213.

Hellstrom, M., Phng, L. K., Hofmann, J. J., Wallgard, E., Coultas, L., Lindblom, P., Alva, J., Nilsson, A. K., Karlsson, L., Gaiano, N. et al. (2007). Dll4 signalling through Notch1 regulates formation of tip cells during angiogenesis. *Nature* **445**, 776-780.

Herrick, S. E. and Mutsaers, S. E. (2004). Mesothelial progenitor cells and their potential in tissue engineering. *Int. J. Biochem. Cell Biol.* **36**, 621-642.

High, F. A., Lu, M. M., Pear, W. S., Loomes, K. M., Kaestner, K. H. and Epstein, J. A. (2008). Endothelial expression of the Notch ligand Jagged1 is required for vascular smooth muscle development. *Proc. Natl. Acad. Sci. USA* **105**, 1955-1959.

Hong, K. U., Reynolds, S. D., Watkins, S., Fuchs, E. and Stripp, B. R. (2004). Basal cells are a multipotent progenitor capable of renewing the bronchial epithelium. *Am. J. Pathol.* **164**, 577-588.

Huppert, S. S., Le A., Schroeter, E. H., Mumm, J. S., Saxena, M. T., Milner, L. A. and Kopan, R. (2000). Embryonic lethality in mice homozygous for a processing-deficient allele of Notch1. *Nature* **405**, 966-970.

Ijpenberg, A., Perez-Pomares, J. M., Guadix, J. A., Carmona, R., Portillo-Sanchez, V., Macias, D., Hohenstein, P., Miles, C. M., Hastie, N. D. and Munoz-Chapuli, R. (2007). Wt1 and retinoic acid signaling are essential for stellate cell development and liver morphogenesis. *Dev. Biol.* **312**, 157-170.

Ito, T., Udaka, N., Yazawa, T., Okudela, K., Hayashi, H., Sudo, T., Guillemot, F., Kageyama, R. and Kitamura, H. (2000). Basic helix-loop-helix transcription factors regulate the neuroendocrine differentiation of fetal mouse pulmonary epithelium. *Development* **127**, 3913-3921.

Jin, S., Hansson, E. M., Tikka, S., Lanner, F., Sahlgren, C., Farnebo, F., Baumann, M., Kalimo, H. and Lendahl, U. (2008). Notch signaling regulates platelet-derived growth factor receptor-beta expression in vascular smooth muscle cells. *Circ. Res.* **102**, 1483-1491.

Kimura, J. and Deutsch, G. H. (2007). Key mechanisms of early lung development. *Pediatr. Dev. Pathol.* **10**, 335-347.

Kong, Y., Glickman, J., Subramaniam, M., Shahsafaei, A., Allamneni, K. P., Aster, J. C., Sklar, J. and Sunday, M. E. (2004). Functional diversity of notch family genes in fetal lung development. *Am. J. Physiol. Lung Cell Mol. Physiol.* **286**, L1075-L1083.

Kopan, R. and Ilagan, M. X. (2009). The canonical notch signaling pathway: unfolding the activation mechanism. *Cell* **137**, 216-233.

Krebs, L. T., Xue, Y., Norton, C. R., Shutter, J. R., Maguire, M., Sundberg, J. P., Gallahan, D., Closson, V., Kitajewski, J., Callahan, R. et al. (2000). Notch signaling is essential for vascular morphogenesis in mice. *Genes Dev.* **14**, 1343-1352.

Lavine, K. J., Long, F., Choi, K., Smith, C. and Ornitz, D. M. (2008). Hedgehog signaling to distinct cell types differentially regulates coronary artery and vein development. *Development* **135**, 3161-3171.

Lee, J., Basak, J. M., Demehri, S. and Kopan, R. (2007). Bi-compartmental communication contributes to the opposite proliferative behavior of Notch1-deficient hair follicle and epidermal keratinocytes. *Development* **134**, 2795-2806.

Liu, H., Kennard, S. and Lilly, B. (2009). NOTCH3 expression is induced in mural cells through an autoregulatory loop that requires endothelial-expressed JAGGED1. *Circ. Res.* **104**, 466-475.

Liu, Y., Pathak, N., Kramer-Zucker, A. and Drummond, I. A. (2007). Notch signaling controls the differentiation of transporting epithelia and multiciliated cells in the zebrafish pronephros. *Development* **134**, 1111-1122.

Ma, X., Renda, M. J., Wang, L., Cheng, E. C., Niu, C., Morris, S. W., Chi, A. S. and Krause, D. S. (2007). Rbm15 modulates Notch-induced transcriptional activation and affects myeloid differentiation. *Mol. Cell. Biol.* **27**, 3056-3064.

Mailleux, A. A., Kelly, R., Veltmaat, J. M., De Langhe, S. P., Zaffran, S., Thiery, J. P. and Bellusci, S. (2005). Fgf10 expression identifies parabronchial smooth muscle cell progenitors and is required for their entry into the smooth muscle cell lineage. *Development* **132**, 2157-2166.

Morimoto, M. and Kopan, R. (2009). rtTA toxicity limits the usefulness of the SP-C-rtTA transgenic mouse. *Dev. Biol.* **325**, 171-178.

Murtaugh, L. C., Stanger, B. Z., Kwan, K. M. and Melton, D. A. (2003). Notch signaling controls multiple steps of pancreatic differentiation. *Proc. Natl. Acad. Sci. USA* **100**, 14920-14925.

Nakayama, K., Satoh, T., Igari, A., Kageyama, R. and Nishida, E. (2008). FGF induces oscillations of Hes1 expression and Ras/ERK activation. *Curr. Biol.* **18**, R332-R334.

Noseda, M., McLean, G., Niessen, K., Chang, L., Pollet, I., Montpetit, R., Shahidi, R., Dorovini-Zis, K., Li, L., Beckstead, B. et al. (2004). Notch activation results in phenotypic and functional changes consistent with endothelial-to-mesenchymal transformation. *Circ. Res.* **94**, 910-917.

Noseda, M., Fu, Y., Niessen, K., Wong, F., Chang, L., McLean, G. and Karsan, A. (2006). Smooth muscle alpha-actin is a direct target of Notch/CSL. *Circ. Res.* **98**, 1468-1470.

Peitz, M., Pfannkuche, K., Rajewsky, K. and Edenhofer, F. (2002). Ability of the hydrophobic FGF and basic TAT peptides to promote cellular uptake of recombinant Cre recombinase: a tool for efficient genetic engineering of mammalian genomes. *Proc. Natl. Acad. Sci. USA* **99**, 4489-4494.

Perl, A. K., Wert, S. E., Nagy, A., Lobe, C. G. and Whitsett, J. A. (2002). Early restriction of peripheral and proximal cell lineages during formation of the lung. *Proc. Natl. Acad. Sci. USA* **99**, 10482-10487.

Perl, A. K., Wert, S. E., Loudy, D. E., Shan, Z., Blair, P. A. and Whitsett, J. A. (2005). Conditional recombination reveals distinct subsets of epithelial cells in trachea, bronchi, and alveoli. *Am. J. Respir. Cell Mol. Biol.* **33**, 455-462.

Plopper, C. G., Suverkropp, C., Morin, D., Nishio, S. and Buckpitt, A. (1992). Relationship of cytochrome P-450 activity to Clara cell cytotoxicity. I. Histopathologic comparison of the respiratory tract of mice, rats and hamsters after parenteral administration of naphthalene. *J. Pharmacol. Exp. Ther.* **261**, 353-363.

Proweller, A., Wright, A. C., Horng, D., Cheng, L., Lu, M. M., Lepore, J. J., Pear, W. S. and Parmacek, M. S. (2007). Notch signaling in vascular smooth muscle cells is required to pattern the cerebral vasculature. *Proc. Natl. Acad. Sci. USA* **104**, 16275-16280.

Que, J., Wilm, B., Hasegawa, H., Wang, F., Bader, D. and Hogan, B. L. (2008). Mesothelium contributes to vascular smooth muscle and mesenchyme during lung development. *Proc. Natl. Acad. Sci. USA* **105**, 16626-16630.

Rawlins, E. L. and Hogan, B. L. (2006). Epithelial stem cells of the lung: privileged few or opportunities for many? *Development* **133**, 2455-2465.

Rawlins, E. L., Ostrowski, L. E., Randell, S. H. and Hogan, B. L. (2007). Lung development and repair: contribution of the ciliated lineage. *Proc. Natl. Acad. Sci. USA* **104**, 410-417.

Reynolds, S. D., Zemke, A. C., Giangreco, A., Brockway, B. L., Teisanu, R. M., Drake, J. A., Mariani, T., Di P. Y., Taketo, M. M. and Stripp, B. R. (2008). Conditional stabilization of beta-catenin expands the pool of lung stem cells. *Stem Cells* **26**, 1337-1346.

Rock, J. R., Onaitis, M. W., Rawlins, E. L., Lu, Y., Clark, C. P., Xue, Y., Randell, S. H. and Hogan, B. L. (2009). Basal cells as stem cells of the mouse trachea and human airway epithelium. *Proc. Natl. Acad. Sci. USA* **106**, 12771-12775.

Sakata, Y., Xiang, F., Chen, Z., Kiriyama, Y., Kamei, C. N., Simon, D. I. and Chin, M. T. (2004). Transcription factor CHF1/Hey2 regulates neointimal formation in vivo and vascular smooth muscle proliferation and migration in vitro. *Arterioscler. Thromb. Vasc. Biol.* **24**, 2069-2074.

Shan, L., Aster, J. C., Sklar, J. and Sunday, M. E. (2007). Notch-1 regulates pulmonary neuroendocrine cell differentiation in cell lines and in transgenic mice. *Am. J. Physiol. Lung Cell Mol. Physiol.* **292**, L500-L509.

Shaw, P. A., Catchpole, I. R., Goddard, C. A. and Colledge, W. H. (2008). Comparison of protein transduction domains in mediating cell delivery of a secreted CRE protein. *Biochemistry* **47**, 1157-1166.

Sisson, T. H., Hansen, J. M., Shah, M., Hanson, K. E., Du, M., Ling, T., Simon, R. H. and Christensen, P. J. (2006). Expression of the reverse tetracycline-transactivator gene causes emphysema-like changes in mice. *Am. J. Respir. Cell Mol. Biol.* **34**, 552-560.

Stenmark, K. R. and Abman, S. H. (2005). Lung vascular development: implications for the pathogenesis of bronchopulmonary dysplasia. *Annu. Rev. Physiol.* **67**, 623-661.

Tanigaki, K., Han, H., Yamamoto, N., Tashiro, K., Ikegawa, M., Kuroda, K., Suzuki, A., Nakano, T. and Honjo, T. (2002). Notch-RBP-J signaling is involved in cell fate determination of marginal zone B cells. *Nat. Immunol.* **3**, 443-450.

Timmerman, L. A., Grego-Bessa, J., Raya, A., Bertran, E., Perez-Pomares, J. M., Diez, J., Aranda, S., Palomo, S., McCormick, F., Izpisua-Belmonte, J. C. et al. (2004). Notch promotes epithelial-mesenchymal transition during cardiac development and oncogenic transformation. *Genes Dev.* **18**, 99-115.

Tsao, P. N., Chen, F., Izvolsky, K. I., Walker, J., Kukuruzinska, M. A., Lu, J. and Cardoso, W. V. (2008). Gamma-secretase activation of notch signaling regulates the balance of proximal and distal fates in progenitor cells of the developing lung. *J. Biol. Chem.* **283**, 29532-29544.

Tsao, P. N., Vasconcelos, M., Izvolsky, K. I., Qian, J., Lu, J. and Cardoso, W. V. (2009). Notch signaling controls the balance of ciliated and secretory cell fates in developing airways. *Development* **136**, 2297-2307.

Vooijs, M., Ong, C. T., Hadland, B., Huppert, S., Liu, Z., Korving, J., van den Born, M., Stappenbeck, T., Wu, Y., Clevers, H. et al. (2007). Mapping the consequence of Notch1 proteolysis in vivo with NIP-CRE. *Development* **134**, 535-544.

Wada, A. M., Smith, T. K., Osler, M. E., Reese, D. E. and Bader, D. M. (2003). Epicardial/Mesothelial cell line retains vasculogenic potential of embryonic epicardium. *Circ. Res.* **92**, 525-531.

Wang, W., Prince, C. Z., Hu, X. and Pollman, M. J. (2003). HRT1 modulates vascular smooth muscle cell proliferation and apoptosis. *Biochem. Biophys. Res. Commun.* **308**, 596-601.

White, A. C., Xu, J., Yin, Y., Smith, C., Schmid, G. and Ornitz, D. M. (2006). FGF9 and SHH signaling coordinate lung growth and development through regulation of distinct mesenchymal domains. *Development* **133**, 1507-1517.

White, A. C., Lavine, K. J. and Ornitz, D. M. (2007). FGF9 and SHH regulate mesenchymal Vegfa expression and development of the pulmonary capillary network. *Development* **134**, 3743-3752.

Wilm, B., Ipenberg, A., Hastie, N. D., Burch, J. B. and Bader, D. M. (2005). The serosal mesothelium is a major source of smooth muscle cells of the gut vasculature. *Development* **132**, 5317-5328.

Xu, Y., Liu, S., Yu, G., Chen, J., Xu, X., Wu, Y., Zhang, A., Dowdy, S. F. and Cheng, G. (2008). Excision of selectable genes from transgenic goat cells by a protein transducible TAT-Cre recombinase. *Gene* **419**, 70-74.

Yin, Y., White, A. C., Huh, S. H., Hilton, M. J., Kanazawa, H., Long, F. and Ornitz, D. M. (2008). An FGF-WNT gene regulatory network controls lung mesenchyme development. *Dev. Biol.* **319**, 426-436.

Yoshiura, S., Ohtsuka, T., Takenaka, Y., Nagahara, H., Yoshikawa, K. and Kageyama, R. (2007). Ultradian oscillations of Stat, Smad, and Hes1 expression in response to serum. *Proc. Natl. Acad. Sci. USA* **104**, 11292-11297.

Yu, K., Xu, J., Liu, Z., Sosic, D., Shao, J., Olson, E. N., Towler, D. A. and Ornitz, D. M. (2003). Conditional inactivation of FGF receptor 2 reveals an essential role for FGF signaling in the regulation of osteoblast function and bone growth. *Development* **130**, 3063-3074.

Zhang, Y., Huang, G., Shornick, L. P., Roswit, W. T., Shipley, J. M., Brody, S. L. and Holtzman, M. J. (2007). A transgenic FOXJ1-Cre system for gene inactivation in ciliated epithelial cells. *Am. J. Respir. Cell Mol. Biol.* **36**, 515-519.

Zhang, Y., Goss, A. M., Cohen, E. D., Kadzik, R., Lepore, J. J., Muthukumaraswamy, K., Yang, J., DeMayo, F. J., Whitsett, J. A., Parmacek, M. S. et al. (2008). A Gata6-Wnt pathway required for epithelial stem cell development and airway regeneration. *Nat. Genet.* **40**, 862-870.

Zhou, B., Ma, Q., Rajagopal, S., Wu, S. M., Domian, I., Rivera-Feliciano, J., Jiang, D., von Gise, A., Ikeda, S., Chien, K. R. et al. (2008). Epicardial progenitors contribute to the cardiomyocyte lineage in the developing heart. *Nature* **454**, 109-113.